PHYSICAL REVIEW C VOLUME 12, NUMBER 6 DECEMBER 1975

# Total $(p,n)$ reaction cross-section measurements on $^{50}Ti$, $^{54}Cr$, and $^{59}Co$

S. Kailas, S. K. Gupta, M. K. Mehta, S. S. Kerekatte, and L. V. Namjoshi
*Nuclear Physics Division, Bhabha Atomic Research Centre, Bombay-400 085, India*

N. K. Ganguly and S. Chintalapudi
*Variable Energy Cyclotron Project, Bhabha Atomic Research Centre, Bombay-400 085, India*

(Received 12 May 1975)

The total $(p,n)$ reaction cross sections, integrated over the $4\pi$ solid angle and summed over all neutron groups, for $^{50}Ti$, $^{54}Cr$, and $^{59}Co$ have been measured as a function of proton energy in the energy range 3.0–4.9, 2.2–5.2, and 2.0–5.1 MeV in 5 keV steps, respectively. No strong isobaric analog resonances were seen in the data. The fluctuations in the excitation functions were analyzed to extract $\langle\Gamma\rangle_{av}$ values using the "counting of maxima" method. The excitation functions, averaged over 100 keV energy interval reveal prominent intermediate width structures in the case of $^{50}Ti$. All the three excitation functions were averaged over suitable energy intervals and compared with the total reaction cross sections calculated utilizing the optical model. The data on $^{59}Co$ and $^{54}Cr$ agreed, while the data on $^{50}Ti$ indicated a marked discrepancy with these optical model calculations. In the latter case, detailed Hauser-Feshbach (HF) and Hauser-Feshbach-Moldauer (HFM) calculations were carried out. The HFM calculations fit the data quite well. The importance of $\sigma(p,n)$ measurements in determining the imaginary potential of the optical model at sub-Coulomb energies has been indicated.

[NUCLEAR REACTIONS $^{54}Cr(p,n)$, $E$=2.2–5.2 MeV; $^{50}Ti(p,n)$, $E$=3.0–4.9 MeV; $^{59}Co(p,n)$, $E$=2–5.1 MeV measured $\sigma(E)$; extracted $\langle\Gamma\rangle_{av}$; optical model and Hauser-Feshbach analyses.]

## I. INTRODUCTION

The $(p, n)$ reactions on medium-weight nuclei are useful in studying the isobaric analog states[1] in the compound nucleus and in determining the proton optical model parameters.[2-4] Generally, for these nuclei the $(p, n)$ channel is open at proton bombarding energies well below the Coulomb barrier. It is also generally expected that at these energies the total reaction cross section could be well approximated by the $(p, n)$ reaction cross section.[5,6] This is because all other charged particle channels, though energetically open, would be inhibited by the Coulomb barrier in those channels. If this is so, the measurement of the $(p, n)$ reaction cross section and comparison with the reaction cross section calculated through the optical model would provide a method for determining the optical model parameters for target plus proton system at these low energies. The more conventional method of finding these through elastic scattering differential cross-section measurement would not be suitable at these energies, as the elastic scattering at forward angles will be dominated by the Coulomb scattering and at backward angles the contribution from compound elastic may be comparable to the potential scattering.

The present measurements of total $(p, n)$ reaction cross sections (integrated over the $4\pi$ solid angle and summed over all neutron groups) on $^{50}Ti$, $^{54}Cr$, and $^{59}Co$ were undertaken with a view to study the excitation functions to determine the optical model parameters for the target plus proton system and to determine the relevant parameters for any prominent isobaric analog resonance,[7] if present. In recent years experimental results have been reported which have indicated the presence of intermediate structure in excitation functions.[8] It would be interesting to look for such structures in the $(p, n)$ reactions. In order to serve all of these purposes the excitation functions were measured with fine (~2–4 keV) resolution and small energy steps (5 keV). The comparison with the optical model and testing for the presence of any gross structure would then require proper averaging of the data. The preliminary results of this work were reported earlier.[9]

## II. EXPERIMENTAL PROCEDURE AND RESULTS

The targets used in the experiment were $^{50}Ti$ (2% $^{46}Ti$, 1.8% $^{47}Ti$, 17.8% $^{48}Ti$, 2% $^{49}Ti$, 76.4% $^{50}Ti$ in the form of $TiO_2$), $^{54}Cr$ (0.11% $^{50}Cr$, 4.01% $^{52}Cr$, 1.79% $^{53}Cr$, 94.1% $^{54}Cr$ in the form of $Cr_2O_3$), and $^{59}Co$ (100% natural). They were prepared by evaporating these materials in vacuum on to thick Ta backing. The target thickness in all the three cases was 2 to 4 keV for 4-MeV protons. The analyzed proton beam from the 5.5-MeV Van de Graaff accelerator at Trombay was collimated on the target which itself served as the Faraday cup. The target was located in the center of a $4\pi$ geometry neutron counter.[10] The excitation function was measured in 5-keV steps from threshold upto 5-MeV proton energy in all the three cases. In the case of $^{50}$Ti target, the excitation function was measured upto 4.9 MeV only because of the $^{48}$Ti-$(p, n)^{48}$V ($^{48}$Ti is 18% in the target used) reaction channel opening up around that energy. The proton current was measured by a current integrator (1% accuracy).[11] The efficiency of the neutron counter is known to an accuracy of 7%.[12] In all the measurements, the background correction was obtained by measuring the yield when the Ta backing was turned around to face the beam. It was found to be of the order of 1% at all energies, except at energies very near the threshold where it became comparable to the yield.

The target thickness in terms of energy loss was determined in each case from the shift in the edge of the spectrum due to the back scattered 2-MeV $\alpha$ particles from the blank tantalum and from the tantalum covered with the target material.[13] A silicon surface barrier detector mounted at 160° with respect to the incident beam was used in these measurements. The total shift in energy will be equal to $\Delta E(1+\sec 20°)$, where $\Delta E$ is the target thickness in terms of energy loss for $E$ which is the mean of the incident and scattered $\alpha$ particle energies.

The absolute maximum error in the $(p, n)$ cross section is estimated to be not more than ±20%, comprised of these errors: the target thickness estimation, 15%; target nonuniformity, 5%; the efficiency of the neutron counter, 7%; and the charge measurement, 1%. The error due to counting statistics is less than ±2%. However, the relative point to point error is ±5%, mainly because

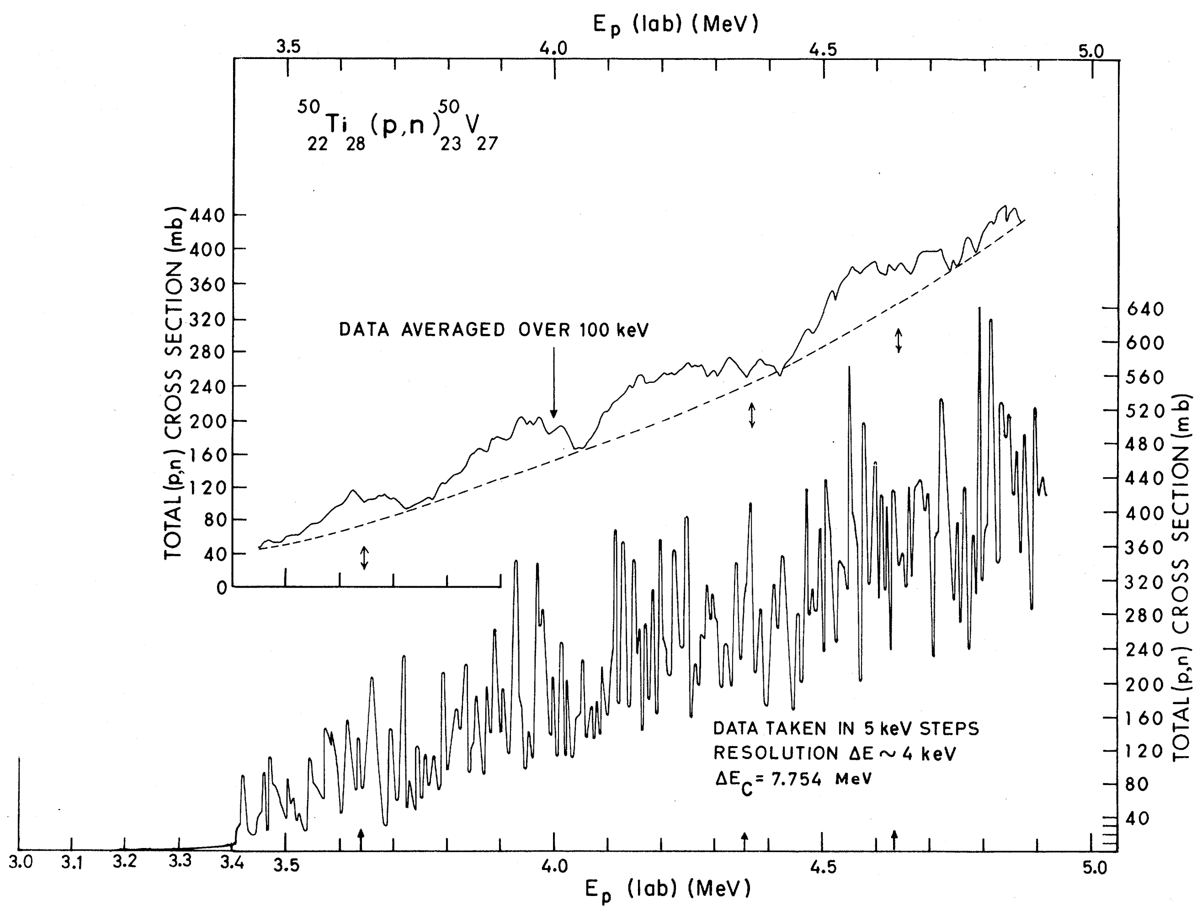


FIG. 1. The total $(p,n)$ cross section (fine resolution and ~100 keV averaged data) for the $^{50}$Ti$(p,n)^{50}$V reaction as a function of the incident proton energy in MeV (lab system). Arrows indicate the expected positions of IARs based on the Coulomb energy shift $\Delta E_C = 7.754$ MeV. Dotted line on the averaged data is drawn through the valleys to bring out the gross structure if present.

of target nonuniformity.

The fine resolution excitation functions in all the three cases are shown in Figs. 1–3. The $^{59}$Co($p$, $n$)-$^{59}$Ni data agree well with the work done with thick targets by Johnson *et al.*[14] when averaged suitably to match their target thickness. The $^{54}$Cr($p$, $n$)-$^{54}$Mn cross section, averaged over suitable energy interval, agrees at low energies with that of Ref. 14. At higher energies there are deviations.

The excitation functions (Figs. 1–3) in all the three cases, exhibited structures with widths of the order of 10–15 keV. Isobaric analog resonances are not very prominently seen except for one or two cases. One or more narrow resonances are present where the isobaric analog resonances (IAR) are expected. However, the presence of equally strong narrow resonances all over the excitation functions indicates that the IARs are not of special significance. The presence of a grosser structure (100 to 150 keV) is indicated in all the three cases to a varying degree, when the data are averaged over 100-keV energy intervals. In the case of Co and Cr targets, the gross structures can be directly correlated with the presence of groups of expected IARs. A number of IARs together, when averaged over 100-keV intervals, appear as one wide structure. However, in the case of $^{50}$Ti, four broad structures are seen which are remarkable in terms of the periodicity and the uniformity. Only three IARs are expected in this range of bombarding energy and three of the observed gross structures more or less correlate with them. However, an interpretation of these wide structures in terms of the isobaric analog states themselves is not possible because of the large observed widths, as well as the presence of one more broad structure which cannot be accounted for in terms of an expected IAR.

## III. ANALYSIS

### A. Fine structure

As pointed out in the Introduction, the excitation functions were measured with fine resolution in order to bring out the isobaric analog resonances if present. No significantly strong IAR was observed and hence no resonance analysis was necessary. The observed width and density of the fine structure in general may represent the Ericson fluctuations[15] as the significant statistical parameter

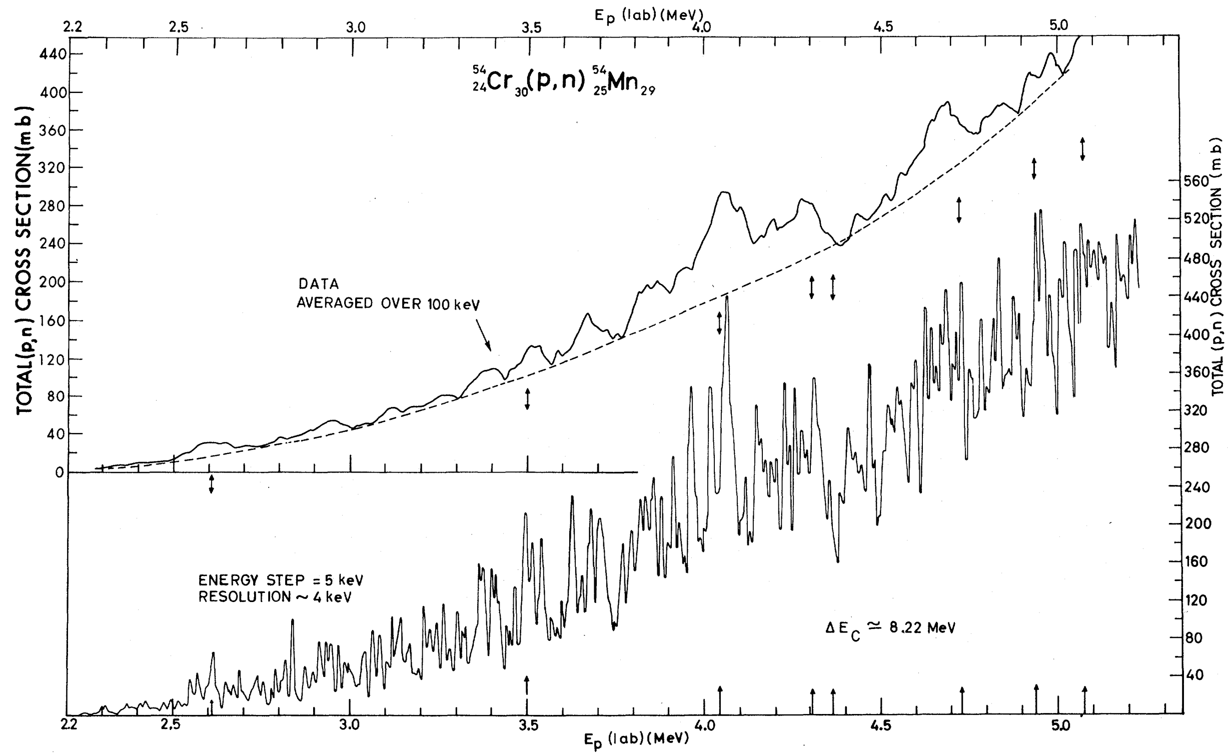


FIG. 2. The total ($p$,$n$) cross section (fine resolution and ~100 keV averaged data) for the $^{54}$Cr($p$,$n$)$^{54}$Mn reaction as a function of the incident proton energy in MeV (lab system). Arrows indicate the expected positions of IARs based on the Coulomb energy shift $\Delta E_C = 8.22$ MeV. Dotted line on the averaged data is drawn through the valleys to bring out the gross structure if present.

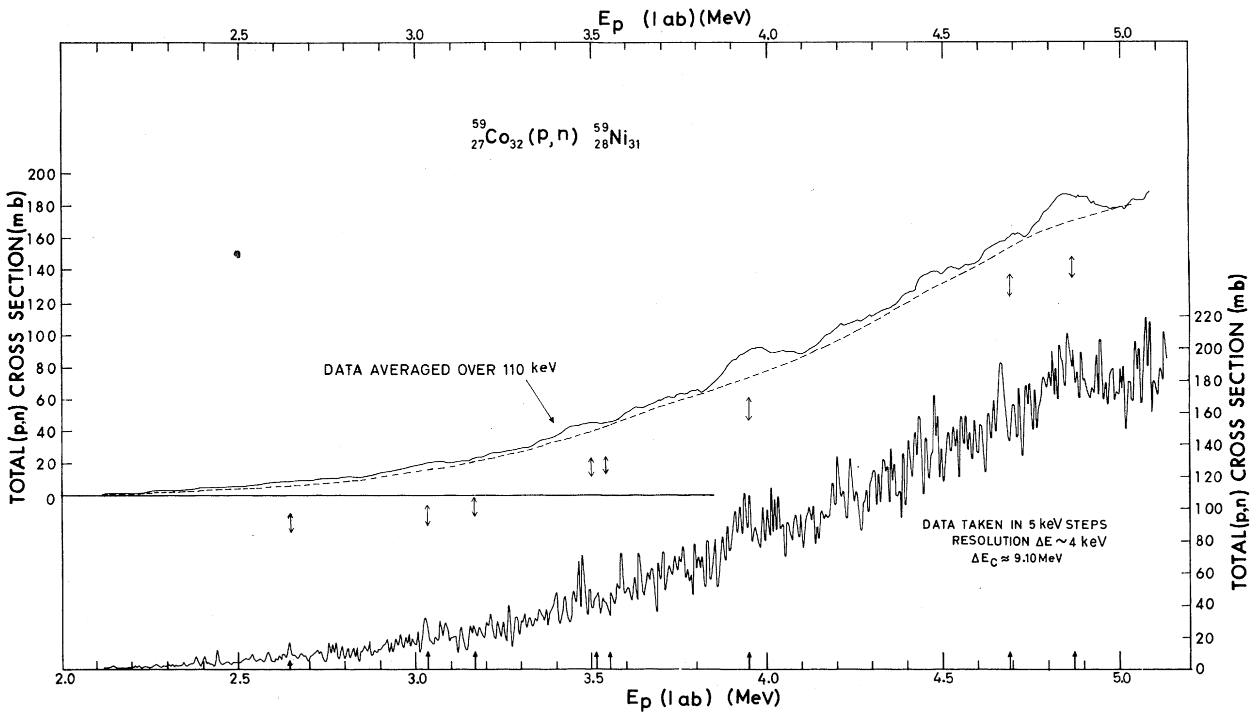


FIG. 3. The total $(p,n)$ cross section (fine resolution and ~100 keV averaged data) for the $^{59}Co(p,n)^{59}Ni$ reaction as a function of the incident proton energy in MeV (lab system). Arrows indicate the expected positions of IARs based on the Coulomb energy shift $\Delta E_C = 9.10$ MeV. Dotted line on the averaged data is drawn through the valleys to bring out the gross structure if present.

$\langle\Gamma\rangle_{av}/D$ in the present case is greater than unity. Out of a number of methods available in literature[16] to extract the value of $\langle\Gamma\rangle_{av}$ (the average level width), the "counting of maxima" method was used to analyze the data for all the three cases. The corrections due to energy resolution and step size were applied as discussed in Ref. 16. Level density expression given by Gilbert and Cameron[17] was used to get the average level separation $D$ for the three $J$ values most likely to be populated in the three cases. It was significant that the ratio $\langle\Gamma\rangle_{av}/D$ determined this way was much larger than one

TABLE I. Results of the fluctuation analysis of the fine structure. The variables $U$, $a$, $\sigma^2$, $J$, $\rho(U, J)$ are as defined in Ref. 17 and the variable $\langle\Gamma\rangle_{av}$ is as defined in Ref. 16.

| Reaction | Compound nucleus | $U$ (MeV) | $a$ (MeV$^{-1}$) | $\sigma^2$ | $\langle\Gamma\rangle_{av}$ (keV) | $J$ | $\rho(U,J)=1/D$ (levels/keV) | $\langle\Gamma\rangle_{av}/D$ |
|---|---|---|---|---|---|---|---|---|
| | | | | | | $\frac{1}{2}$ | 0.86 | 6.4 |
| $^{50}Ti(p,n)^{50}V$ | 51 | 10.70 | 6.375 | 9.986 | 7.4 ± 1.5 | $\frac{3}{2}$ | 1.47 | 10.9 |
| | | | | | | $\frac{5}{2}$ | 1.72 | 12.7 |
| | | | | | | $\frac{1}{2}$ | 1.20 | 11.76 |
| $^{54}Cr(p,n)^{54}Mn$ | 55 | 10.73 | 6.710 | 10.800 | 9.8 ± 2.0 | $\frac{3}{2}$ | 2.07 | 20.24 |
| | | | | | | $\frac{5}{2}$ | 2.46 | 24.11 |
| | | | | | | 3 | 2.3 | 13.34 |
| $^{59}Co(p,n)^{59}Ni$ | 60 | 11.03 | 6.540 | 11.454 | 5.8 ± 1.2 | 4 | 2.1 | 12.18 |
| | | | | | | 5 | 1.7 | 9.86 |

in all the cases. This justified the fluctuation interpretation of the structure. The results of this analysis are shown in Table I.

### B. Optical model and Hauser-Feshbach analysis

For a compund nuclear process the reaction cross section is given by the Hauser-Feshbach expression (HF) based on the statistical model[18] and when level width fluctuations are taken into account, the cross section is given by Moldauer's formula (HFM),[19] which is a modification of the Hauser-Feshbach approach. When the proton transmission coefficients can be neglected in comparison to the neutron transmission coefficients, the HF or HFM expressions reduce to a simple expression which is the same as that given for the total reaction cross section by the optical model. This approximation would be quite valid at sub-Coulomb energies. This can be seen from the following: Starting with the expression given by Marmier and Sheldon[20] the total ($p$, $n$) cross section, using the Hauser-Feshbach formalism can be written as

$$\sigma_{p,n} = \pi \lambda\!\!\!^{-}_p{}^2 \sum_{J_i,\, j_p,\, l_p} \frac{(2J_i+1)}{(2J_0+1)(2\mathcal{S}_p+1)} \times \frac{T_{l_p j_p}(E_p) \sum_{l_n j_n E_n} T_{l_n j_n}(E_n)}{T_{l_p j_p}(E_p) + \sum_{l_n j_n E_n} T_{l_n j_n}(E_n)}$$

where $J_0$, and $\mathcal{S}_p$ equal the target and the projectile spins, $J_i$ equals the compound nuclear spin, and $T$'s are the transmission coefficients. For the present sub-Coulomb cases, the transmission coefficients for the other open charged particle channels will be even smaller than that for the proton channel and are neglected in writing the above expression. If we make the assumption that $\sum T_{l_n j_n}(E_n) \gg T_{l_p j_p}(E_p)$ which is valid at sub-Coulomb energies and above neutron threshold, and use the fact that $\sum_{J_i}(2J_i+1) = (2J_0+1)(2j_p+1)$, the above expression reduces to

$$\sigma_{p,n} = \pi \lambda\!\!\!^{-}_p{}^2 \sum_{j_p l_p} \frac{(2j_p+1)}{(2\mathcal{S}_p+1)} T_{l_p j_p}(E_p)\,.$$

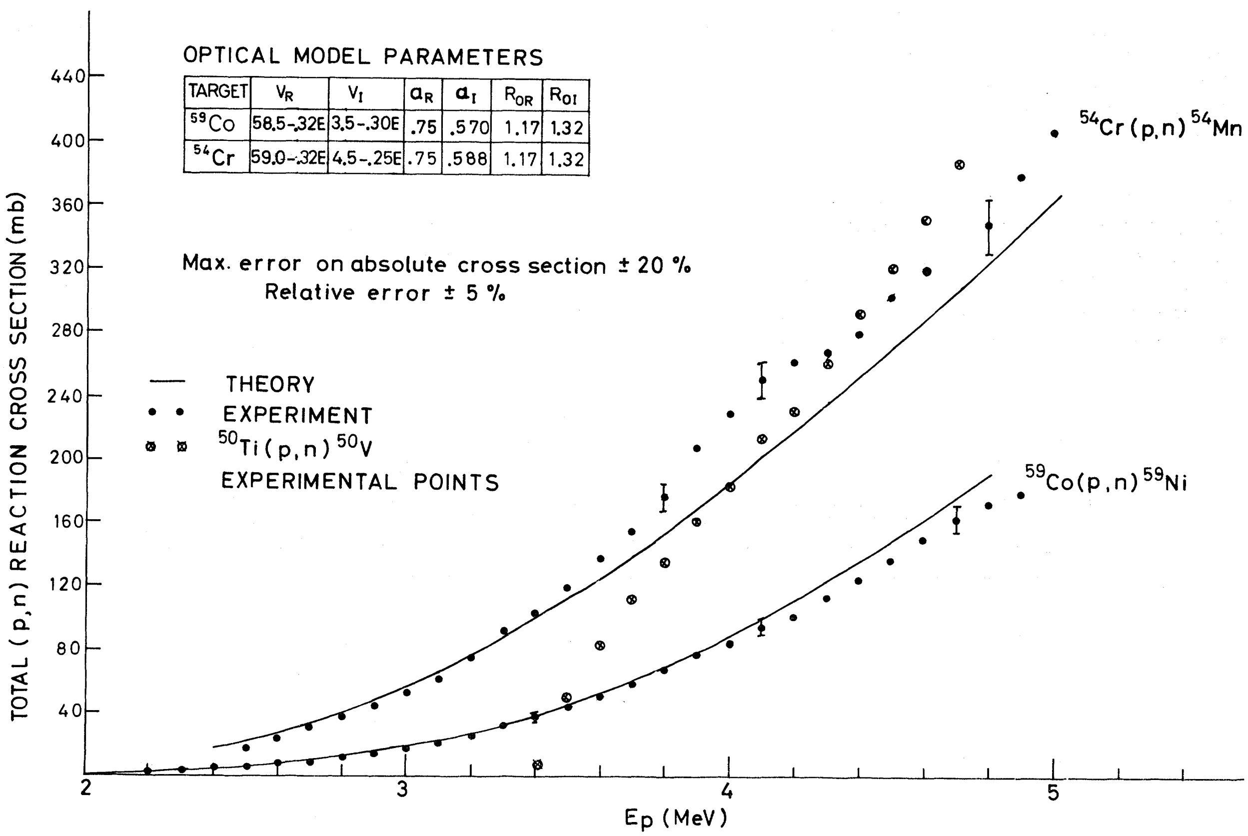


FIG. 4. The optical model fits to $^{54}$Cr($p$,$n$)$^{54}$Mn, $^{59}$Co($p$,$n$)$^{59}$Ni data averaged over an interval of approximately 200–500 keV. The significance of the fits are discussed in the text. Woods-Saxon derivative form factor has been used for the imaginary potential $V_I$. The optical model potentials and form factors are as given in Ref. 22.

Further using the fact $\vec{j}_p = \vec{l}_p + \vec{s}_p$ and $s_p = \frac{1}{2}$ we get

$$\sigma_{p,n} = \pi \lambda_p^2 \sum_{l_p} [(l_p+1)T_{l_p j_{p\uparrow}} + l_p T_{l_p j_{p\downarrow}}],$$

where $j_{p\uparrow} = l_p + \frac{1}{2}$ and $j_{p\downarrow} = l_p - \frac{1}{2}$. The above expression is identical to $\sigma_R$, the reaction cross section calculated using the optical model. The comparison of measured $\sigma(p,n)$ (averaged to smooth out the observed fine structure) directly with the optical model predicted reaction cross section does not require information on the low lying energy levels of the target and residual nuclides, whereas the comparison with the HF or HFM needs this as well as the neutron optical model parameters.

The fine resolution excitation functions for $^{50}$Ti, $^{54}$Cr, and $^{59}$Co were averaged over large energy intervals (~ 200 to 500 keV) and then were compared with the optical model predictions of reaction cross section. The optical model code ABACUS-2 (Ref. 21) was used to calculate the total reaction cross section starting with the optical model parameters given by Becchetti and Greenlees.[22] The imaginary potential $V_I$ was varied suitably to get best fits to Co and Cr data keeping all the other parameters fixed. The fits are shown in Fig. 4. The fits are very good at lower energies in both the cases. The calculated $\sigma_R$ at higher energies in the case of $^{59}$Co is slightly higher than measured $(p,n)$ cross section. This is understandable as near the top of the Coulomb barrier other open channels may start contributing to $\sigma_R$ substantially. The fit to $^{54}$Cr data deviates substantially from the measured data only in the regions where the presence of groups of IARs has resulted in apparent gross structures. The above procedure of varying only the $V_I$ parameter would be justified as the calculation of the reaction cross section would be most sensitive to the value of $V_I$. However, as discussed in Ref. 2, the diffuseness parameter $a_I$ also can be varied to fit the reaction data. In the present analysis the objective was to compare the value of $V_I$ determined here with that determined by Becchetti and Greenlees.[22] In order to do this meaningfully, all the other parameters (including $a_I$) were kept at the same value as that given in Ref. 22. It was possible to fit the data on $^{59}$Co and $^{54}$Cr and determine the value of $V_I$ within ±1 MeV. The parameters which gave the best fits for these cases are listed in Table II. However, in the case of Ti no amount of adjustment of $V_I$ could produce a satisfactory fit. This is evident from the observed steep slope of the averaged $^{50}$Ti-$(p,n)^{50}$V data as indicated in Fig. 4.

In Table II, the parameters obtained by extrapolating downwards the values given in Ref. 22 are also listed. The extrapolation was done assuming the energy dependence also given in Ref. 22. The comparison of the two sets indicates that the values for $V_I$ differ significantly. It was assumed that the energy dependence of the real potential as given in Ref. 22 would still be valid at lower energies. However, it has been indicated that this is not so and the energy dependence becomes large at sub-Coulomb energies.[2] When variation of real potential was tried, it was found that the fits were not sensitive enough to determine the energy dependence of the real potential in this range. On the other hand, for the imaginary potential, it is expected that at these energies, the extrapolation from higher energies would not be valid as the level densities are drastically reduced at these low energies. The fact that the values of $V_I$ determined in this work (~4–5 MeV) are significantly different from those given in Ref. 22, bears this out.

It can be seen from Fig. 4 that the assumption $\sigma_{p,n} \sim \sigma_R$ is valid in the case of $^{59}$Co$(p,n)^{59}$Ni reaction and to a certain extent for the $^{54}$Cr$(p,n)^{54}$Mn reaction and meaningful values of optical parameter $V_I$ can be obtained. However, in the case of the $^{50}$Ti target the fact that the optical model calculations could not reproduce the data indicates

TABLE II. Optical-model parameters: $V_R$ is the real potential (Woods-Saxon form); $V_I$ is the imaginary potential (derivative Woods-Saxon form); $a_R$, $a_I$ are the diffuseness parameters for real and imaginary potentials; and $R_{0R}$, $R_{0I}$ are the radius parameters for real and imaginary potentials.

| Optical model parameters | $^{54}$Cr Becchetti and Greenlees | $^{54}$Cr Our values | $^{59}$Co Becchetti and Greenlees | $^{59}$Co Our values |
|---|---|---|---|---|
| $V_R$ | 59.2–0.32$E$ | 59.0–0.32$E$ | 58.8–0.32$E$ | 58.5–0.32$E$ |
| $V_I$ | 13.1–0.25$E$ | 4.5–0.25$E$ | 12.8–0.25$E$ | 3.5–0.30$E$ |
| $a_R$ | 0.75 | 0.75 | 0.75 | 0.75 |
| $a_I$ | 0.588 | 0.588 | 0.57 | 0.570 |
| $R_{0R}$ | 1.17 | 1.17 | 1.17 | 1.17 |
| $R_{0I}$ | 1.32 | 1.32 | 1.32 | 1.32 |

that the above assumption is not valid. Because of the large difference in the ground state spin of $^{50}$Ti and spins of low lying states[23] of $^{50}$V, the $(p, n)$ reaction is inhibited and compound elastic scattering becomes the dominant reaction channel at energies near the threshold. Hence, the assumption $\sigma_{p,n} \sim \sigma_R$ fails in this case. So the more accurate, HF and HFM calculations were carried out to fit the $^{50}$Ti$(p, n)^{50}$V excitation function. The optical model parameters similar to the ones used by Egan *et al.*[24] were used to get the transmission coefficients. Using the known level schemes[23,25,26] of $^{50}$Ti and $^{50}$V the HF calculations were performed utilizing the expressions given in Ref. 20. The Hauser-Feshbach treatment assumes a uniform distribution of level widths. However, the level widths are expected to follow a Porter-Thomas distribution.[27] Moldauer[19] has taken this statistical nature of the level width distribution into account in deriving the cross section expression averaged over compound nuclear levels. This is the most general expression for cross section for a particular reaction channel. A code HAFEC[28] was written to calculate independently the HF and HFM predicted cross sections. The calculations were performed with the following assumptions: The partial widths were assumed to have a Porter-Thomas distribution with one degree of freedom. The value of Moldauer parameter $Q$ used,[19] was zero, justified by the fact that the excitation energy was high and $\langle\Gamma\rangle/D \gg 1$. Details of these calculations are described in Ref. 28. For simple HF calculation, the expression in Ref. 20 was used. The theoretical fits (HF and HFM) to the (averaged) measured $^{50}$Ti$(p, n)^{50}$V excitation function are shown in Fig. 5. The fit obtained with HFM is the best and closely reproduces the experimental data.

### C. Strength function analysis

In comparing theories of various nuclear models certain average properties of nuclear levels are of considerable interest. One such property is the average strength of levels, as measured by the strength function (SFN) $= \langle \gamma^2 \rangle_{av}/D$, where $\langle \gamma^2 \rangle_{av}$ is the average reduced width for a particular reaction channel of levels with the same quantum numbers $\pi$ and $J$. $D$ is the average spacing of such levels.

The Coulomb and angular momentum effects can be removed from the cross section and excitation curves by introducing the SFN. Following a method similar to that of Johnson and Kernell[2] the proton strength functions were calculated for the three cases measured in the present work utilizing the Coulomb function code COULOMB[29] to calculate the penetrabilities. The SFNs (in units of $10^{-14}$ cm) calculated are as follows: for $^{50}$Ti, $2.4 \pm 0.80$; $^{54}$Cr, $3.47 \pm 0.48$; and $^{59}$Co, $2.22 \pm 0.16$. The errors indicated are due to variation of SFN over the energy range in which they were calculated.

## IV. CONCLUSION

The results of the analysis discussed above show that at these sub-Coulomb energies, extrapolation

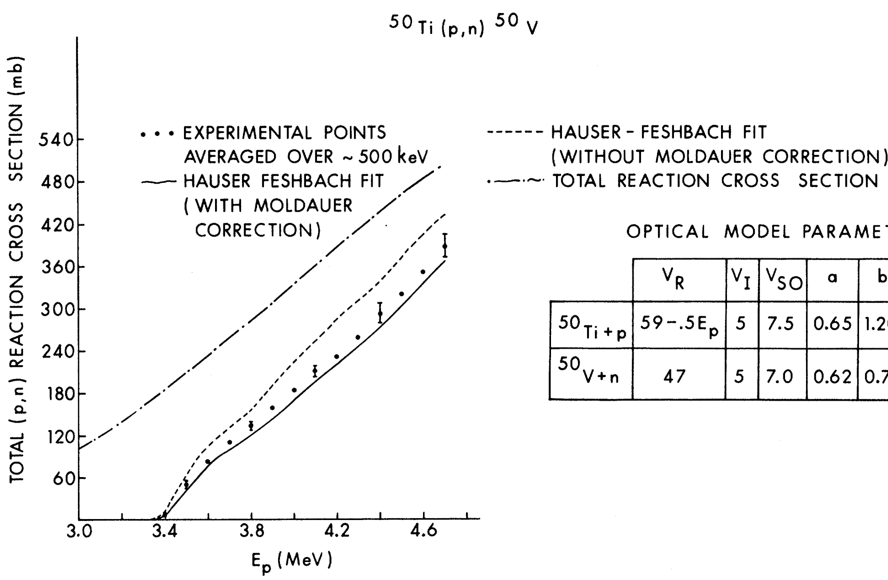


OPTICAL MODEL PARAMETERS

| | $V_R$ | $V_I$ | $V_{SO}$ | a | b | $R_{OR} = R_{OI}$ |
|---|---|---|---|---|---|---|
| $^{50}$Ti + p | $59 - .5E_p$ | 5 | 7.5 | 0.65 | 1.20 | 1.25 |
| $^{50}$V + n | 47 | 5 | 7.0 | 0.62 | 0.71 | 1.30 |

FIG. 5. Hauser-Feshbach and Hauser-Feshbach-Moldauer theoretical fits to $^{50}$Ti$(p,n)^{50}$V averaged data. The Gaussian form factor has been used for the imaginary potential $V_I$. The optical model potentials and form factors are similar to that given in Ref. 24.

downwards of the optical potentials determined from the analysis of elastic scattering data at higher energy may not be quite valid. This is particularly true for the imaginary potential. As discussed earlier elastic scattering cross sections at these energies would be completely dominated by Coulomb scattering and will not be sensitive to the nuclear optical potentials. Our work here indicates that $(p, n)$ reaction cross sections measurement would be a more suitable method to determine these potentials for sub-Coulomb energies.

From the comparison of the optical model reaction cross section with the Hauser-Feshbach-Moldauer calculations in the case of $^{50}$Ti, it is clear that when all "$l$" values do not contribute to the $(p, n)$ reaction, because of the specific properties of the nuclear levels involved, the optical model reaction cross section fails to be a good approximation to the $(p, n)$ cross section. In such a case the compound elastic channel becomes a major contributor to the reaction cross section.

The most interesting feature of the data is the appearance of intermediate width structures in the case of the $^{50}$Ti$(p, n)^{50}$V reaction. The structures are striking because of their regularity in positions, widths, and heights. In order to trace the origin of these broad structures and their probable interpretation as doorway states in the entrance channel, it would be necessary to measure the excitation function for other open channels, i.e., $^{50}$Ti$(p, p)^{50}$Ti, $^{50}$Ti$(p, p')^{50}$Ti, and $^{50}$Ti$(p, \alpha)^{47}$ Sc and look for correlations with the $(p, n)$ data. However, if these structures are due to doorway states in the exit channel, the confirmation of them through $^{50}$V$+n$ experiments will not be feasible because of the target difficulties. Theoretical interpretation of these structures in terms of possible doorway configurations would be meaningful only when existence of these structures in a specific channel can be confirmed or some properties like the spin and parity can be measured.

## V. ACKNOWLEDGMENTS

The help of Mr. C. V. Fernandez and Mr. V. V. Tambvekar at various stages of the experiment is gratefully acknowledged. The authors also thank Mr. Y. P. Viyogi for his help in the optical model calculations and Dr. B. Lal for providing a copy of his computer programme on $(p, n\gamma)$ calculations using Hauser-Feshbach theory. Thanks are also due the Van de Graaff accelerator crew for their cooperation.

[1] *Isobaric Spin in Nuclear Physics*, edited by J. D. Fox and and D. Robson (Academic, New York, 1966).
[2] C. H. Johnson and R. L. Kernell, Phys. Rev. C 2, 639 (1970).
[3] R. D. Albert, Phys. Rev. 115, 925 (1959).
[4] S. Kailas, M. K. Mehta, and S. K. Gupta, Nucl. Phys. Solid State Phys. (India) 16B, 31 (1973).
[5] C. H. Johnson, A. Galonsky, and J. P. Ulrich, Phys. Rev. 109, 1243 (1958).
[6] J. P. Schiffer and L. L. Lee, Jr., Phys. Rev. 109, 2098 (1958).
[7] K. K. Sekharan and M. K. Mehta, Phys. Rev. C 6, 2304 (1972).
[8] P. E. Hodgson, *Nuclear Reactions and Nuclear Structure* (Clarendon, Oxford, 1971).
[9] M. K. Mehta, S. Kailas, L. J. Kanetkar, S. S. Kerekatte, S. K. Gupta, S. Chintalapudi, and N. K. Ganguly, Bull. Am. Phys. Soc. 18, 658 (1973).
[10] K. K. Sekharan, M.Sc. thesis, Bombay University, 1966 (unpublished).
[11] S. K. Gupta, Nucl. Instrum. Methods 60, 323 (1968).
[12] S. K. Gupta and S. S. Kerekatte, BARC Report No. 579, 1971 (unpublished).
[13] M. Balakrishnan, S. Kailas, S. S. Kerekatte, and M. K. Mehta, Nucl. Phys. Solid State Phys. (India) 17B, 309 (1974).
[14] C. H. Johnson, A. Galonsky, and C. N. Inskeep, ORNL Report No. ORNL-2910, 1960 (unpublished), pp. 25–28.
[15] T. Ericson and T. Mayer-Kuckuk, Annu. Rev. Nucl. Sci. 16, 183 (1966).
[16] M. G. Braga Marcazzon and L. Milazzo Colli, Prog. Nucl. Phys. 2, 145 (1969).
[17] A. Gilbert and A. G. W. Cameron, Can. J. Phys. 43, 1446 (1965).
[18] W. Hauser and H. Feshbach, Phys. Rev. 87, 366 (1952).
[19] P. A. Moldauer, Rev. Mod. Phys. 36, 1079 (1964); P. A. Moldauer, C. A. Engelbrecht, and G. J. Duffy, ANL Report No. ANL-6978, 1964 (unpublished).
[20] P. Marmier and E. Sheldon, *Physics of Nuclei and Particles* (Academic, New York, 1970), Vol. 2, Chap. 14.
[21] E. H. Auerbach, ABACUS-II. Program Operation and Input Description, BNL Report No. BNL-6562, 1962.
[22] F. D. Becchetti and G. W. Greenlees, Phys. Rev. 182, 1190 (1969).
[23] S. K. Gupta, S. Saini, L. V. Namjoshi, and M. K. Mehta, Pramāna 5, 37 (1975).
[24] J. J. Egan, K. K. Sekharan, G. C. Dutt, J. E. Wiest, and F. Gabbard, Phys. Rev. C 1, 1767 (1970).
[25] C. M. Lederer, J. M. Hollander, and I. Perlman, *Table of Isotopes* (Wiley, New York, 1968).
[26] R. Del Vecchio, W. W. Daehnick, D. L. Dittmer, and Y. S. Park, Phys. Rev. C 3, 1989 (1971).
[27] C. E. Porter and R. G. Thomas, Phys. Rev. 104, 483 (1956).
[28] S. Kailas, S. K. Gupta, and M. K. Mehta, BARC Report No. I-360, 1975 (unpublished).
[29] L. V. Namjoshi and S. K. Gupta (unpublished).